Research Article

LUMINESCENCE
The Journal of Biological and Chemical Luminescence

Received: 19 January 2008, Revised: 14 April 2008, Accepted: 28 April 2008, Published online 11 September 2008 in Wiley Interscience

(www.interscience.wiley.com) DOI 10.1002/bio.1066

A novel biosensor for bovine serum albumin based on fluorescent self-assembled sandwich bilayers

Xiangying Sun*, Bin Liu and Fei He

ABSTRACT: Fluorescent dyes butyl rhodamine B were assembled via a DL-cystenine intermediate onto quartz wafers whose surface had first adsorbed gold nanoparticles. Hence self-assembled sandwich bilayers with nanocomposite structure were constructed which can be used as a biosensor for bovine serum albumin. The biosensor-based self-assembled monolayers (SAMs) are regenerable and have high sensitivity, five orders of magnitude higher than that of bulk solution phase sensing. The effects of existing forms of dyes on the fluorescence spectra of bilayers in the presence of bovine serum albumin were investigated. Copyright © 2008 John Wiley & Sons, Ltd.

Keywords: self-assembled bilayers; fluorescence sensor; gold nanoparticles; butyl rhodamine B; bovine serum albumin

Introduction

The process of self-assembly provides a powerful tool for generating molecular films of biological molecules on a wide variety of substrates. The simplicity and flexibility of self-assembled monolayers (SAMs) and the possibility of controlling biomolecule surface orientation allow SAMs to play an important task in the design of artificial biomolecular recognition devices (1, 2). As the field of nanotechnology rapidly evolves, interest in the organized assembly of nanoscale structures into functional materials has greatly intensified. Because of their large specific surface area and amplification for the sensing signals, nanoparticles are becoming frequent targets for use as components in molecular machines as well as miniaturized and specialized sensors (3–7). SAMs of thiolates on colloidal gold clusters are therefore ideal substrates for investigating nanoparticle microfabrications (8–11), as possibilities exist for further modification. The interest in fluorescent chemosensors is growing as they provide sensitive and selective assays to recognize and evaluate species and concentrations of substrates of concern. It is therefore of basic significance to examine fluorescent sensing on the basis of nanoparticle modifications on SAMs.

Conventional fluorescence analysis in liquid phase can only be used once and also contaminate sample solutions. In our laboratory, we developed an interfacial fluorescence analytical method by combining SAMs technology with a fluorescence analytical method. Our experiments showed that indirectly assembling fluorophores onto a gold surface could efficiently eliminate fluorescence quenching by gold, and therefore fluorescent sensors based on SAMs might be fabricated. This method was effective in diminishing the sample volume with a view to on-chip analysis and has higher analytical sensitivity than fluorescence analysis in liquid phase, and thus has promising prospects in the fields of fluorescence analysis and chemical sensors (12–14).

Herein a novel fluorescent biosensor for bovine serum albumin based on gold nanoparticle SAMs has been explored. Gold nanoparticles were first assembled onto a quartz surface, forming a Quartz/AuNP nanocomposite structure. Fluorescent dyes butyl rhodamine B (BRB) were indirectly assembled onto the surface of Quartz/AuNP via a DL-cystenine (Cys) intermediate; fluorescent bilayers of Quartz/AuNP/Cys/BRB were then constructed and could be used as a biosensor for bovine serum albumin (BSA). The sensor-based SAMs are regenerable and have high sensitivity, five orders of magnitude higher than that of bulk solution phase sensing. The effects of existing forms of dyes on the fluorescence spectra of bilayers in the prescence of bovine serum albumin were investigated.

Experimental

Apparatus and reagents

Corrected fluorescence spectra were recorded on a Varian fluorescence spectrophotometer. The slits for excitation and emission monochromators were both 5 nm. The angle between the quartz wafer plane and incident excitation light was set at 50° to ensure maximum efficiency for collecting emitting light, while avoiding reflection light interference (Scheme 1). A 1×1 cm quartz cell was employed for recording fluorescence spectra. Absorption spectra were recorded on a Tu-1810PC spectrophotometer.

All chemicals were of analytical grade or above. Aqueous solutions were prepared using water from a Millipore Milli-Q system (18 MΩ cm).

Preparation of fluorescent self-assembled sandwich bilayers (Quartz/AuNP/Cys/BRB)

Silanization of quartz wafers. Quartz wafers, $1 \times 1 \times 0.001$ cm, were immersed in solution ($HF:H_2SO_4:H_2O = 1:1:3$ v/v/v) for 1 min,

* Correspondence to: X. Sun, College of Materials Science and Engineering, Huaqiao University, Quanzhou 362021, People's Republic of China. E-mail: liumy@hqu.edu.cn

College of Materials Science and Engineering, Huaqiao University, Quanzhou 362021, People's Republic of China

LUMINESCENCE
The Journal of Biological and Chemical Luminescence

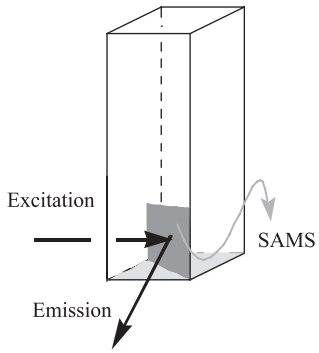

Scheme 1. Systematic diagram of the attachment for this experiment.

washed ultrasonically in ethanol for 10 min and dried in nitrogen. The quartz wafers were immersed into hot piranha solution (H_2SO_4:H_2O_2 = 7:3 v/v) for 1 h, then washed ultrasonically in ethanol for 10 min, dried in nitrogen, and heated at 120°C for 30 min in an oven. The treated quartz wafers were finally immersed in γ-aminopropyltriethoxysilane (APES) toluene solution for 3 h, and washed and dried.

Deposition of colloidal gold particles on silanized quartz wafers. All glassware used for preparation of the colloids was thoroughly washed with aqua regia (HCl:HNO_3, 3:1 v/v) and rinsed extensively in water. Gold colloids were prepared by the reduction of $HAuCl_4$ with sodium citrate in water, as previously reported (15).

Each silanized quartz wafer was dipped in a 2 mL freshly prepared gold colloidal suspension for 12 h. The wafers were then removed from the suspension and left to dry in nitrogen for 10 min.

Preparation of fluorescent self-assembled sandwich bilayers (Quartz/AuNP/Cys/BRB). Quartz wafers modified by colloidal gold particles (Quartz/AuNP) were immersed in 0.01 mol/L cysteine solution, pH 11.4, for 6 h, leading to the quartz wafers combined with cysteine. Quartz/AuNP/Cys/BRB was fabricated by immersing the cysteine-modified quartz wafers (Quartz/AuNP/Cys) in 0.0001 mol/L solution of butyl rhodamine B, pH 5.7, for 12 h. The assembly process is depicted in Scheme 2. Butyl rhodamine B was electrostatically bound to cysteine and fluorescent self-assembled quartz wafers were obtained.

Results and discussion

Characterization of butyl rhodamine B in solution

Butyl rhodamine B is a kind of basic dye. The pH of solution affects the fluorescence spectra of butyl rhodamine B. There were poor fluorescent characteristics in strong acidic solution (pH < 1.5) and intense fluorescence emission at pH > 3. Therefore, we chose dye solution of pH 5.7 for assembly. The concentration of dye has effects on the existing forms of butyl rhodamine B. For dilute dye solution (≤0.0001 mol/L), there is strong fluorescence emission from the monomer, which presents an emission band centred at 580 nm, fluorescence intensity increased with increasing concentration (Fig. 1a). However, for concentrated dye solution (≥0.005 mol/L), which has non- or poor emission capacity because of dye-aggregation to dimers, the fluorescence intensity decreased with increasing concentration and the emission band was red-shifted to 627 nm with increasing concentration of the dye (Fig. 1b). Figure 2 shows the absorption spectra of butyl rhodamine B, there is an intense band at 557 nm and a shoulder at 517 nm. The intense band at 557 nm is attributed to the 0–0 absorption band corresponding to the s_1–s_0 transition, which is directed parallel to the long axis of the chromophore. The appearance of another band at 517 nm with increasing concentration of butyl rhodamine B may be attributed to the dimer or aggregates of rhodamine (16–18). Indeed, it has been found that butyl rhodamine B dyes have a tremendous propensity to aggregate, even at a very low concentration (5×10^{-6} mol/L). From the above discussion, it is clear that the spectral characterization of butyl rhodamine B is concentration-dependent.

The interaction between butyl rhodamine B and bovine serum albumin (BSA)

Experiments on the interaction between butyl rhodamine B and bovine serum albumin in solution were carried out. Changes in the fluorescence spectra of butyl rhodamine B in the presence of

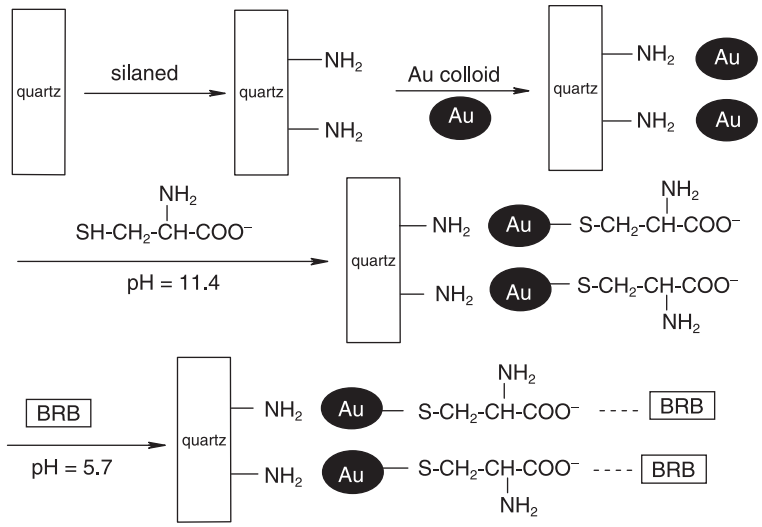

Scheme 2. Fabricating process for Quartz/AuNP/Cys/BRB.

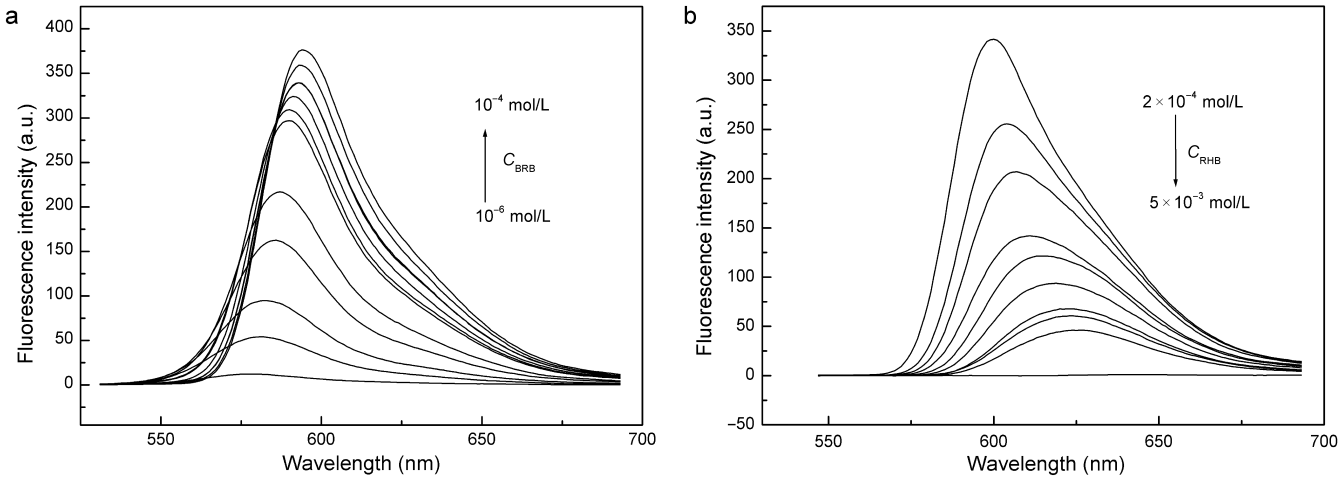

Figure 1. Fluorescence spectra of butyl rhodamine B with (a) lower concentrations and (b) higher concentrations.

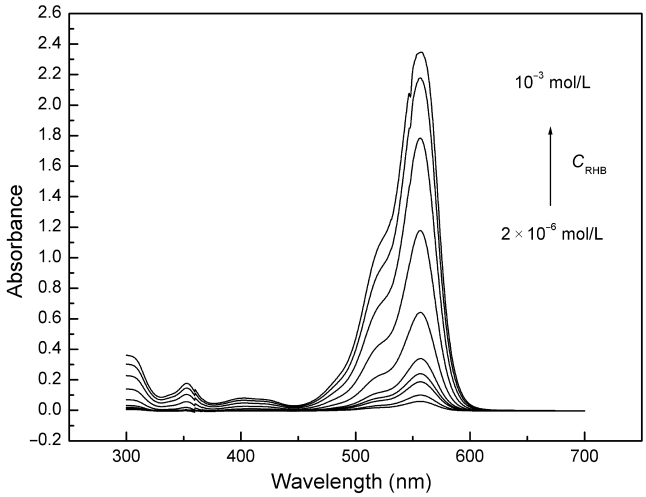

Figure 2. Absorption spectra of butyl rhodamine B with different concentrations.

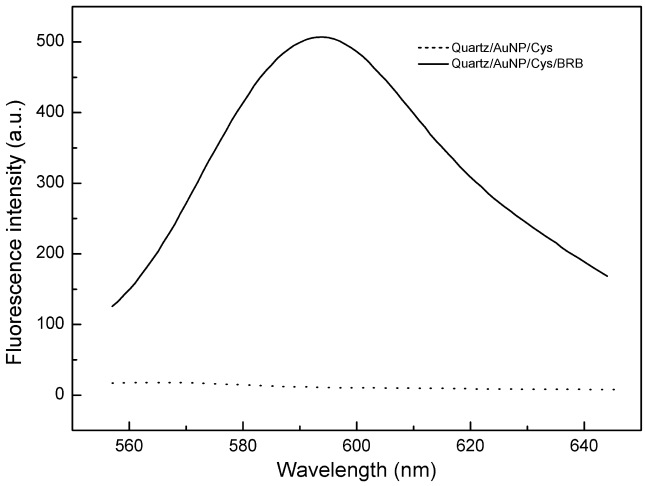

Figure 3. Fluorescence emission spectra of Quartz/AuNP/Cys/BRB and Quartz/AuNP/Cys.

BSA were dependent on existing forms of the dyes. When the dye molecules mainly existed as monomers, fluorescence intensity decreased with the increasing concentration of BSA, while when the dye molecules mainly existed as dimer, fluorescence intensity increasing with increasing concentration of BSA, which may be explained by the dye dimer being transformed to monomers in the presence of BSA. As BSA affects the fluorescence intensity of butyl rhodamine B, BSA can be detected based on this, but with low sensitivity of the detection limit of 1.131×10^{-4} g/L. We therefore assembled butyl rhodamine B onto the surface of quartz wafers to increase the sensitivity of recognition for BSA.

Spectral properties of Quartz/AuNP/Cys/BRB wafers

Figure 3 shows the surface fluorescence spectra of Quartz/AuNP/Cys/BRB and Quartz/AuNP/Cys wafers at 400 nm excitation. It was found that the Quartz/AuNP/Cys/BRB wafer exhibits the characteristic fluorescent emission peak of rodamine B molecules and the Quartz/AuNP/Cys wafer was non-fluorescent, further confirming that butyl rhodamine B had been assembled onto the quartz surface. The intermediate of cysteine in BRB–Cys–AuNP–quartz prevented direct contact of the dye molecules with the gold surface and hence the interactions between fluorescing molecules and the free electrons in the metal that resulted in the rapid transfer of energy and relaxation responsible for gold-surface fluorescence quenching (19). The fluorescence emission of Quartz/AuNP/Cys/BRB wafer peaked at 597 nm, which was a little blue-shifted compared to that of butyl rhodamine B dimer bulk solution.

Interfacial sensing of Quartz/AuNP/Cys/BRB for bovine serum albumin

As butyl rhodamine B can interact with BSA in solution, we studied the changes of fluorescence spectra of Quartz/AuNP/Cys/BRB wafers in the presence of BSA, and found that the fluorescence intensity increased and the emission bands had a little blue-shifted with increasing BSA (Fig. 4). There was a non-linear relationship between fluorescent intensity and concentration of BSA; the detection limit (3 SD/k) was 3.2×10^{-10} g/L, five orders of magnitude lower than that of the bulk solution-phase detection limit of 1.131×10^{-4} g/L. It is thus shown that the sensitivity of interfacial analysis based on SAMs was greatly enhanced compared to that of the corresponding solution-phase analysis.

LUMINESCENCE
The Journal of Biological and Chemical Luminescence

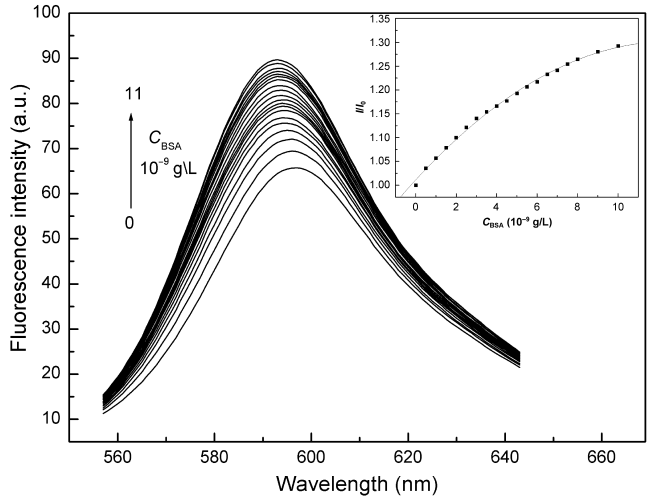

Figure 4. Fluorescence spectra for Quartz/AuNP/Cys/BRB in the presence of BSA. Inset shows line plots for the relative fluorescence intensity of Quartz/AuNP/Cys/BRB vs. BSA concentration. I_0 and I, fluorescence intensity in the absence and presence, respectively, of BSA.

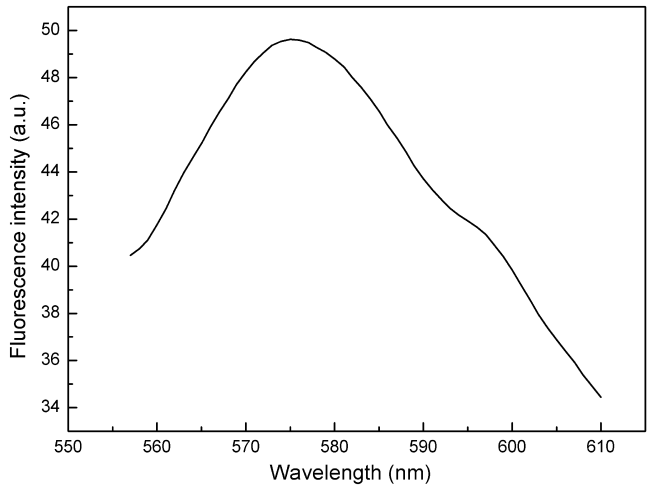

Figure 5. Fluorescence spectra for Quartz/AuNP/Cys/BRB prepared with 0.00001 mol/L butyl rhodamine B.

The fluorescence intensity changes of Quartz/AuNP/Cys/BRB wafers in the presence of BSA were similar to those of butyl rhodamine B dimer in solution. We assumed that the dye molecules existed as dimers in a multilayer, which was confirmed by the following experiments. We immersed Quartz/AuNP/Cys wafers in very dilute butyl rhodamine B solution of 10^{-6} mol/L, and the intense fluorescence emission of prepared multilayers peaked at 575 nm and very weak emission peaked at ca. 595 nm (Fig. 5). This may be ascribed to the dye molecules existing mainly as monomers in the film. Fluorescence intensity at 575 nm decreased with increasing BSA, which was similar to that of the dye monomer in solution acted with BSA. From the above-mentioned, we concluded that the existing forms of butyl rhodamine B in bilayers would be concentration-dependent; the dye molecules assembled onto the quartz wafers modified by colloidal gold particles are more likely to encourage dimer formation at lower concentrations, which affects the photophysical properties of films and interaction between Quartz/AuNP/Cys/BRB wafers and BSA.

Fluorescence reversibility

Reversibility is an important parameter of a sensor. It is desirable that, after the analysis, the sensor–analyte interaction could be readily reversed. In this process, the analyte (BSA herein) was released from the sensor membrane, so that the sensor was restored to its original form and ready for the next measurement. We examined the reversibility of the Quartz/AuNP/Cys/BRB wafer by following its fluorescence variations. Quartz/AuNP/Cys/BRB wafers were put into BSA solution and the fluorescence intensity increased with immersion time. When the wafer was again put into 1 mol/L sodium citrate solution for 20 min and then into ultrapure water, the fluorescence was efficiently regenerated, near to its original intensity. Therefore, a reversibility was observed with the fluorescence of this Quartz/AuNP/Cys/BRB.

Interference experiments

Our preliminary experiments showed that the presence of <10 equivalents of Cu^{2+}, five equivalents of Fe^{3+}, did not lead to interference of the fluorimetric detection by 10% change in the emission intensity. Monosaccharides and common ions such as K^+, Na^+ and Zn^{2+} had no influence on the assays.

We also studied the interactions between Quartz/AuNP/Cys/BRB and DNA, and found that the fluorescence intensity increased with increasing DNA concentration. The bilayers can be also used as a sensor for DNA at the interface. Further experiments on the interactions between the fluorescent bilayers and DNA are in progress.

Conclusion

Novel fluorescent self-assembled sandwich bilayers, Quartz/AuNP/Cys/BRB, were constructed based on SAMs nanocomposite structure via a DL-cystenine intermediate. The film was found to be highly fluorescent and can be used as a biosensor for bovine serum albumin at the interface. The biosensor-based SAMs are regenerable and have good stability, with a high sensitivity five orders of magnitude higher than that of the bulk solution phase sensing. The existing forms of butyl rhodamine B in bilayers would be concentration-dependent, and the dye molecules assembled onto the quartz wafers modified by colloidal gold particles are more likely to encourage the dimer formation at a lower concentration, which affects the photophysical properties of films and the interaction between Quartz/AuNP/Cys/BRB wafers and BSA.

Acknowledgements

This work was supported by the National Natural Science Foundation of China (Grant No. 20575023), the Natural Science Foundation of Fujian Province (Grant Nos. D0710017 and D0810016), the International Cooperative Foundation of Fujian Province (Grant No. 2006I0021) and the Foundation of Overseas-Chinese Affairs Office of the State Council of China (Grant No. 06QZR10).

References

1. Ferretti S, Paynter S, Russell DA, Sapsford KE, Richardson DJ. Self-assembled monolayers: a versatile tool for the formulation of biosurfaces. *Trends Anal. Chem*. 2000; **19**: 530–540.
2. Revell DJ, Knight JR, Blyth DJ, Haines AH, Russell DA. Self-assembled carbohydrate monolayers: formation and surface selective molecular recognition. *Langmuir* 1998; **14**: 4517–4524.

3. Huang CC, Chiu SH, Huang YF, Chang HT. Aptamer-functionalized gold nanoparticles for turn-on light switch detection of platelet-derived growth factor. *Anal. Chem*. 2007; **79**: 4798–4804.
4. Roy D, Fendler J. Reflection and absorption techniques for optical characterization of chemically assembled nanomaterials. *Adv. Mater*. 2004; **16**: 479–508.
5. Shervedani RK, Mozaffari SA. Copper(II) nanosensor based on gold cysteamine self-assembled monolayer functionalized with salicylaldehyde. *Anal. Chem*. 2006; **78**: 4957–4963.
6. Nagle L, Ryan D, Cobbe S, Fitzmaurice D. Templated nanoparticle assembly on the surface of a patterned nanosphere. *Nano Lett*. 2003; **3**: 51–53.
7. Simonian AL, Good TA, Wang SS, Wild JR. Nanoparticle-based optical biosensors for the direct detection of organophosphate chemical warfare agents and pesticides. *Anal. Chim. Acta* 2005; **534**: 69–77.
8. Fleming MS, Walt DR. Stability and exchange studies of alkanethiol monolayers on gold-nanoparticle-coated silica microspheres. *Langmuir* 2001; **17**: 4836–4843.
9. Boal AK, Iihan F, Derouchey JE, Thurn-Albrecht T, Russell TP, Rotello VM. Self-assembly of nanoparticles into structured spherical and network aggregates. *Nature* 2000; **404**: 746–748.
10. Flink S, van Veggel FCJM, Reinhoudt DN. Functionalization of self-assembled monolayers on glass and oxidized silicon wafers by surface reactions. *J. Phys. Org. Chem*. 2001; **14**: 407–415.
11. Pompano RR, Wortley PG, Moatz LM, Tognarelli DJ, Kittredge KW, Leopold MC. Crown ether-metal 'sandwiches' as linking mechanisms in assembled nanoparticle films. *Thin Solid Films* 2006; **510**: 311–319.
12. Sun XY, Liu B, Weng WT, Jiang YB. A novel fluorometric detection of Cu^{2+} based on self-assembled bilayers. *Talanta* 2004; **62**: 1035–1040.
13. Sun XY, Liu B, Weng WT, Jiang YB. An extremely sensitive monoboronic acid based fluorescent sensor for glucose. *Anal. Chim. Acta* 2004; **515**: 285–290.
14. Sun XY, Liu B, Weng WT. Preparation and properties of fluorescent self-assembled bilayer membrane. *Chem. J. Chin. Univ*. 2005; **26**: 1030–1034.
15. Frens G. Controlled nucleation for the regulation of the particle size in monodisperse gold suspensions. *Nat. Phys. Sci*. 1973; **241**: 20–22.
16. Ray K, Nakahara H. Adsorption of sulforhodamine dyes in cationic Langmuir–Blodgett films: spectroscopic and structural studies. *J. Phys. Chem. B* 2002; **106**: 92–100.
17. Martínez V, López Arbeloa F, Bañuelos Prieto J, López Arbeloa I. Characterization of rhodamine 6G aggregates intercalated in solid thin films of laponite clay 2 fluorescence spectroscopy. *J. Phys. Chem. B* 2005; **109**: 7443–7450.
18. Zhao J, Jensen L, Sung JH, Zou SL, Schatz GC, van Dauyne RP. Interaction of plasmon and molecular resonances for rhodamine 6G adsorbed on silver nanoparticles. *J. Am. Chem. Soc*. 2007; **129**: 7647–7656.
19. Ishida A, Majima T. Surface plasmon enhanced fluorescence measurement on flat and constructed gold surfaces. *Analyst* 2000; **125**: 535–540.